Global Change Biology (2004) **10,** 1133–1145, doi: 10.1111/j.1365-2486.2004.00784.x

Climate controls on vegetation phenological patterns in northern mid- and high latitudes inferred from MODIS data

XIAOYANG ZHANG, MARK A. FRIEDL, CRYSTAL B. SCHAAF, ALAN H. STRAHLER
Department of Geography, Center for Remote Sensing, Boston University, 675 Commonwealth Avenue, Boston, MA 02215, USA

Abstract

Recent studies using both field measurements and satellite-derived-vegetation indices have demonstrated that global warming is influencing vegetation growth and phenology. To accurately predict the future response of vegetation to climate variation, a thorough understanding of vegetation phenological cycles and their relationship to temperature and precipitation is required. In this paper, vegetation phenological transition dates identified using data from the moderate-resolution imaging spectroradiometer (MODIS) in 2001 are linked with MODIS land surface temperature (LST) data from the northern hemisphere between 35°N and 70°N. The results show well-defined patterns dependent on latitude, in which vegetation greenup gradually migrates northward starting in March, and dormancy spreads southward from late September. Among natural vegetation land-cover types, the growing-season length for forests is strongly correlated with variation in mean annual LST. For urban areas, the onset of greenup is 4–9 days earlier on average, and the onset of dormancy is about 2–16 days later, relative to adjacent natural vegetation. This difference (especially for urban vs. forests) is apparently related to urban heat island effects that result in both the average spring temperature and the mean annual temperature in urban areas being about 1–3 °C higher relative to rural areas. The results also indicate that urban heat island effects on vegetation phenology are stronger in North America than in Europe and Asia. Finally, the onset of forest greenup at continental scales can be effectively described using a thermal time-chilling model, which can be used to infer the delay or advance of greenup onset in relation to climatic warming at global scale.

Keywords: vegetation phenology, MODIS, land surface temperature, urban heat island, phenology model

Revised 25 July 2003; revised version received and accepted 8 September 2003

Introduction

Phenological observations and calendars have been used in agriculture for thousands of years, and phenological records have a history going back to the early 1700s in Europe (e.g. Sparks & Carey, 1995) and the 1800s in Japan (Lauscher, 1978). More recently, the utility of phenology for analyzing climatic and ecological changes has prompted substantial new scientific interest in seasonal-to-decadal-scale dynamics in vegetation (e.g. Myneni *et al*., 1997; Schwartz, 1999; Lucht *et al*., 2002). Field observations of species-level phenophases have been successfully associated with local and regional climatic variations occurring over several decades (Fitter *et al*., 1995; Lechowicz & Koike, 1995; Kramer, 1996; Beaubien & Freeland, 2000; Chmielewski & Rötzer, 2001), and long-term records of budburst and flowering dates show strong associations with interannual variation in air temperatures. Warmer spring temperatures have advanced flowering dates by about 4 days per °C (Fitter *et al*., 1995) and leaf unfolding by about 3.2–3.6 days per °C in Europe (Kramer, 1996; Rötzer & Chmielewski, 2000). On average, springtime phenological events have changed by 2.3 days per decade globally (Parmesan & Yohe, 2003). Similarly, the

Correspondence: Xiaoyang Zhang, Department of Geography, Center for Remote Sensing, Boston University, 675 Commonwealth Avenue, Boston, MA 02215, USA, e-mail: zhang@crsa.bu.edu

growing-season length (GSL) of deciduous broadleaf forests during the period from 1900 to 1987 increased by about 5 days as a result of a 1 °C increase in mean annual temperature in the eastern United States (White *et al.*, 1999).

Using normalized difference vegetation index (NDVI) data derived from the advanced very high-resolution radiometer (AVHRR) between 1981 and 1991, Myneni *et al.* (1997) estimated an advance of 8 ± 3 days in the onset of spring and an increase of 12 ± 4 days in GSL in northern latitudes (45–70°N). Similarly, comparison of average AVHRR-NDVI values from July 1981 to December 1999 has shown that the duration of growing seasons has increased by as much as 18 days in Europe and Asia, and by 12 days in northern North America (Zhou *et al.*, 2001).

Urban heat island effects also provide evidence regarding how vegetation phenology will respond to future global warming. Such effects can be evaluated based on observed temperature differences between urban and rural areas. For example, recent field observations have demonstrated that the onset of flowering in urban areas has advanced by about 4 days on average relative to rural areas (Roetzer *et al.*, 2000), and by as much as 17 days for some species (Franken, 1955). Using AVHRR-NDVI data in the eastern United States, White *et al.* (2002) found that greenup occurs 5.7 days earlier, dormancy occurs 2.0 days later, and that the GSL is 7.6 days longer in urban areas relative to deciduous broadleaf forests in rural areas.

Because of the sensitivity of vegetation phenology to climate variation in general, and temperature changes in particular, it is important to understand how climate forcing affects vegetation phenology at the ecosystem level. In this context, the aim of this study is to use remote sensing to detect the spatial distribution of vegetation phenology and to quantitatively examine the linkage between phenology and climatic variation in the northern hemisphere between 35°N and 70°N. In particular, we focus on the effect of temperature variability on phenology, and by extension, the potential impact of global warming on vegetation communities. To achieve this goal, we utilize data from the moderate-resolution imaging spectroradiometer (MODIS) in 2001 to identify phenological transition dates globally. The resultant phenological measurements are then related to MODIS land surface temperature (LST) measurements to assess the phenological response of various land-cover types to spatial variability in LST. Finally, a thermal time-chilling model to predict the onset of spring greenup at the level of entire ecosystems is used to quantify the sensitivity of vegetation phenology in mid-latitudes to the effects of global warming.

Data and methods

Data

The MODIS instrument on-board NASA's Terra and Aqua platforms includes seven spectral bands that are explicitly designed for land surface monitoring (Justice *et al.*, 1997). The improved spectral, radiometric, and geometric quality of MODIS data provide an effective means of monitoring global environmental changes. In this study, we used nadir bidirectional reflectance distribution function (BRDF) adjusted reflectance (NBAR) data from MODIS (product MOD43B4 version 3) for the period from January 1 to December 31, 2001. Using daily multiangle surface reflectance observations collected over 16-day periods, the MODIS NBAR product provides surface reflectances in the seven land bands at 1 km spatial resolution (Schaaf *et al.*, 2002). This dataset is ideal for global land surface analysis since view angle effects have been removed and both cloud and aerosol contamination have been minimized. This product also provides a snow and ice flag in its quality assurance (QA) field indicating whether the data were acquired from a snow covered or snow-free surface, depending on which condition was present for the majority of a 16-day period.

Temperature data are essential for understanding the response of vegetation phenology to climate change. The MODIS LST product provides estimates of land surface skin temperature, and is calculated using satellite thermal-infrared measurements for clear-sky pixels with a spatial resolution of 1 km. The accuracy of this product is within 1 °C (Wan *et al.*, 2002). The MODIS MOD11A2 LST product (version 3) provides surface temperatures for 8 day time periods by averaging the daily LST measurements (Wan *et al.*, 2002). To match the temporal scale of the NBAR data and to further reduce the number of missing values (because of cloud cover), the 8-day daytime LST data in 2001 were aggregated to 16 days using QA information from the LST product. If the QA showed that LST data were of good quality for both 8-day periods, the higher value was used in order to avoid residual cloud and atmospheric contamination. If only one LST value with good quality was available, it was selected. To generate an annual time series of LST without missing values for the entire northern mid- and high latitudes, any 16-day period with a missing value was replaced using an average of the preceding and following LST values at that pixel. These LST data calculated from MODIS observations are standard and comparable, although they are not equivalent to the near surface air temperature (Huband & Monteith, 1986).

Land-cover data used in this study were derived from the MODIS land-cover product. The primary land-cover types in this product include 17 land-cover classes following the International Geosphere–Biosphere Program (IGBP) scheme (Friedl *et al*., 2002). To stratify the northern mid- and high latitudes into different climate regimes, a Köppen climate classification map with 0.5° spatial resolution produced by the Food and Agriculture Organization (FAO) was used. This system consists of five major climate groups, with six subgroups and six further subdivisions. Each climate regime is defined according to fixed limits of mean annual and monthly temperature and precipitation. For this work, we used this climate classification to stratify land surfaces according to whether vegetation phenology was dominated by either temperature or precipitation.

Detection of phenological transition dates

Until recently, AVHRR NDVI data were the main remote sensing source for identifying phenological events in vegetation communities at coarse spatial resolution. Unfortunately, the quality of NDVI derived from AVHRR data is limited by a number of factors. Specifically, it tends to saturate at relatively low values of leaf area index on the ground and also includes high levels of noise associated imprecise atmospheric corrections, residual cloud contamination, and view angle biases (e.g. Goward *et al*., 1991). Despite these drawbacks, various methods have been developed to measure the start date of spring greenup and the end date of vegetation growth. Specifically, reported methods include NDVI thresholds (Lloyd, 1990; Fisher, 1994; Markon *et al*., 1995), backward and forward moving windows from the annual cycle of biweekly composted NDVIs (Reed *et al*., 1994), fitting linear segments to NDVI time series in deciduous forests (Duchemin *et al*., 1999), a normalized NDVI ratio in deciduous broadleaf forests in the United States (White *et al*., 1997), and the derivative of NDVI calculated from a moving window with 5-week periods (Moulin *et al*., 1997). More recently, Zhang *et al*. (2003) developed a method to estimate phenological events based on the curvature-change rate for time series of MODIS data. This method has been used in this study because it is ecologically meaningful, able to handle multiple growth cycles, and does not require the use of arbitrarily defined thresholds to identify phenological transition dates.

Processing annual time series of NBAR EVI data. To quantify vegetation activity, the enhanced vegetation index (EVI) has been used instead of the NDVI because it reduces sensitivity to soil and atmospheric effects, and remains sensitive to variation in canopy density where NDVI becomes saturated (Huete *et al*., 2002). For this work, annual time series of EVI were calculated at each pixel from 16-day NBAR data using the formula developed by Huete *et al*. (2002)

$$\mathrm{EVI} = G\frac{\rho_{\mathrm{NIR}} - \rho_{\mathrm{red}}}{\rho_{\mathrm{NIR}} + C_1\rho_{\mathrm{red}} - C_2\rho_{\mathrm{blue}} + L}, \qquad (1)$$

where ρ_{blue}, ρ_{red} and ρ_{NIR} are NBAR values in the MODIS blue, red, and near infrared bands, respectively, L (= 1) is the canopy background adjustment, C_1 (= 6) and C_2 (= 7.5) are aerosol resistance coefficients, and G (= 2.5) is a gain factor.

To analyze vegetation dynamics, it is essential to identify the background EVI associated with leaf off or minimum LAI conditions. Within a phenological cycle, the background EVI is defined as the minimum and stable EVI value for a pixel not related to the effects of clouds and snow. Since cloud cover is explicitly masked in NBAR EVI data, the main factor causing variation in EVI values unrelated to phenology is snow cover, which covers about $47\times10^6\,\mathrm{km}^2$ of land area between December and February in the northern hemisphere (Gutzler & Rosen, 1992). To remove these effects, snow periods are determined using the snow and ice flag retrieved from the NBAR QA data, and the corresponding EVIs are replaced with the most recent snow-free values. This procedure may not completely remove snow effects in pixels with partial snow cover. To further reduce the impact of snow, LST values are also used. If the EVI varies irregularly when LST is less than 5 °C, these values are replaced with the nearest-neighbor values in the time series. This procedure is based on the assumption that vegetation is dormant during periods of very low temperature (e.g. Cannell *et al*., 1985).

Increasing (growth) and decreasing (senescence) periods in annual time series of EVI are determined using a moving window method. Using moving windows composed of five 16-day periods, transitions from increasing to decreasing EVI periods are identified by a change from positive to negative slope, and vice versa. Periods with small increases and decreases in EVI are ignored because they are associated with transient climate effects or data quality instead of seasonal vegetation cycles. Such variations are detected by comparing the local magnitude of EVI with the maximum variation in the corresponding annual EVI. In this way, an arbitrary number of growth cycles are calculated within a given annual time series by identifying periods of sustained EVI increase and decrease.

Identifying transition dates. Field measurements have shown that sigmoidal growth models are effective for

depicting vegetation growth curves as a function of time (or cumulative temperature) (e.g. Ratkowsky, 1983). Hence, a logistic model of vegetation growth is employed here to fit each increasing or decreasing section of EVI time series. The logistic model is implemented using the following expression:

$$\mathrm{EVI}(t) = \frac{c}{1 + e^{a+bt}} + d, \tag{2}$$

where t is time (day of year, DOY), a and b are empirical coefficients associated with the rate of change in EVI, c is the potential maximum EVI value for a given vegetation type, and d represents the background EVI value (Fig. 1). These four curve coefficients (a, b, c and d) for each section of vegetation growth are estimated using the Levenberg–Marquardt method (Press *et al.*, 1997).

Phenological transition dates in a given EVI trajectory are determined using the curvature-change rate (C_{CR}), which is the derivative of the curvature in the function given by Eqn (2):

$$C_{CR} = b^3 cz \left\{ \frac{3z(1-z)(1+z)^3\left[2(1+z)^3 + b^2c^2z\right]}{\left[(1+z)^4 + (bcz)^2\right]^{5/2}} - \frac{(1+z)^2(1+2z-5z^2)}{\left[(1+z)^4 + (bcz)^2\right]^{3/2}} \right\}, \tag{3}$$

where $z = e^{a+bt}$, and transition dates correspond to the times at which the rate of change in curvature of the EVI series exhibits local minima or maximums. During periods when EVI increases (e.g. spring), two maximum values of C_{CR} can be identified that are related to specific phenological transition dates: greenup onset and maturity onset. In contrast, when EVI declines at the end of a cycle (e.g. fall), two minimum values of C_{CR} indicate senescence onset and dormancy onset (Fig. 1). GSL is then easily determined from the difference between dormancy onset and greenup onset. In this study, we focus only on the onset of greenup and the onset of dormancy in relation to temperature and land-cover type.

Quantifying ecosystem level phenological variations and their relation to land-cover type and temperature

Vegetation phenology is controlled by temperature, photoperiod, precipitation, vegetation type, and human activity. In temperate and boreal regions, temperature is the dominant climatic variable related to vegetation phenology (e.g. Cannell & Smith, 1986; White *et al.*, 1997).

Zonal phenology variations with land-cover type and temperature. By using zonal averages, the spatial uncertainty in both phenology and temperature is reduced and latitude-based estimates of daytime solar radiation can be included in analyses. Since our goal is to investigate the response of vegetation phenology to temperature for several key land-cover types, we subdivided the temperature and phenological datasets based on three criteria. First, the MODIS IGBP land-cover types were used to stratify the data to account for the effects of different ecosystems and human activity. To simplify this, IGBP land-cover types were aggregated into seven classes including forests (deciduous broadleaf forests + mixed forests), shrubs (closed shrublands + open shrublands), savannas (woody savannas + savannas), grasses (grasslands), crops (croplands), urban (urban and built-up lands), and naturally vegetated mosaics (forests + shrubs + savannas + grasses). Evergreen needleleaf forests were excluded from this analysis since their phenological signals are more subtle relative to those of the other land-cover types. Second, Köppen climate classes were

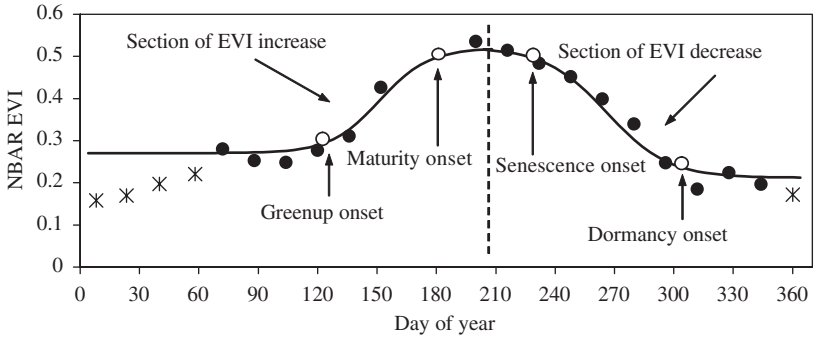

Fig. 1 Pixel-based detection of phenological transition dates for mixed forests in North America. The solid dots indicate NBAR EVI without snow effects, and the stars are the EVI values during snow periods. The solid line is the logistic curve fitted to the NBAR EVI, and white circles are the dates corresponding to the extreme points determined by the curvature-change rate.

used to separate humid climate regions from arid climate regions. This allowed us to distinguish regions dominated by temperature and photoperiod limitations from those limited by water restrictions. Third, only areas with a single annual cycle of phenology were considered since multiple growth cycles are mainly the result of human activity (such as double crops) or seasonal variations in precipitation in semiarid areas.

Zonal averages for phenological transition dates across 1 min (1.85 km) latitude intervals were then computed for all of the selected land-cover types in the humid climate zone. Using the same procedure, we also computed the corresponding mean annual LST for each one-minute zone because phenological events, GSL, and annual net primary productivity are strongly associated with mean annual temperature at continental scales (Lieth, 1975; White *et al*., 1997, 1999, 2002).

Phenology differences between urbanized and rural areas. Phenological data and corresponding LST values were also retrieved for $0.5^\circ \times 0.5^\circ$ (45 km × 56 km at 35°N) cells surrounding urban regions and were used to analyze the effect of urban climates on vegetation phenology. To do this, we calculated the differences in greenup onset (ΔG_d), dormancy onset (ΔD_d), growing-season length (ΔGSL), mean spring LST (January to May, ΔLST_{1-5}), and mean annual LST (ΔLST_a) between urban areas and surrounding natural vegetation. Following White *et al*. (2002), only cells with urban land cover totaling more than 2% of each $0.5 \times 0.5^\circ$ cell were included for this comparison since small urban areas were unlikely to produce significant urban warming.

Spring greenup model at the ecosystem level. To investigate how global warming might influence dates of vegetation greenup at global scales, a model is required. For individual species, various models are available for predicting vegetation greenup. Commonly used models include those based on spring warming, sequential chilling (chilling triggered), thermal time-chilling, and photothermal (light triggered) criteria (Sarvas, 1974; Cannell & Smith, 1983; Hunter & Lechowicz, 1992; Kramer, 1994; Linkosalo, 2000). In the thermal time-chilling model, vegetation is assumed to respond to increased duration of previous chilling by decreasing the requirements of temperature forcing to initiate spring greenup. This model is appropriate for investigating vegetation greenup at continental scales (Botta *et al*., 2000). In this framework, degree-days (DDs) to greenup onset (budburst) can be expressed as an exponential function of the chilling duration (Cannell & Smith, 1983; Cannell *et al*., 1985):

$$T_{DD} = \alpha + \beta e^{\gamma C_d}, \quad (4)$$

where T_{DD} is DDs from a specified date to greenup onset, C_d is the number of chill days (days with temperature less than a threshold) from a given date to the date of greenup onset, and α, β, and γ are coefficients estimated using the Levenberg–Marquardt method.

The correct starting date and an appropriate threshold or base temperature for calculating T_{DD} and C_d are critical to this model. The starting date is usually chosen in late autumn after leaf senescence, so November 1 is often used to calculate C_d and January 1 or February 1 is commonly used for T_{DD} (e.g. Cannell & Smith, 1983; Hunter & Lechowicz, 1992). Because of the fact that both vegetation and climate vary widely at continental to global scales, we used a spatially variable start date of dormancy onset for calculating both T_{DD} and C_d. Choosing a temperature threshold between 0 °C and 5 °C has little effect on the accuracy of DD calculations (Spano *et al*., 1999), and both 0 °C and 5 °C are commonly used (e.g. Cannell *et al*., 1985; Hunter & Lechowicz, 1992; Emberlin *et al*., 2002). Because air temperatures are not available globally, we tested LST thresholds of 0 °C and 5 °C for this purpose.

Results and discussion

Spatial distribution of phenology

Figure 2 presents maps showing the dates for both greenup onset and dormancy onset estimated from MODIS data between 35°N and 70°N in 2001. As expected, the patterns depend strongly on latitude in the mid- to high latitudes, and reveal how greenup onset pushes northward from March to early June, and how dormancy onset spreads southward beginning in late September around 65°N and ending in late November in the southern mid-latitudes. Note that the main period of growth for vegetation in Mediterranean regions and the southwestern United States is in the winter and spring because of heat stress and seasonal precipitation patterns.

Spatial variation in phenology is also associated with land-cover type (Figs 3 and 4). Forests are mainly distributed in humid climatic zones, such as eastern North America and the boreal zone. As a consequence, phenological transition dates for forests vary strongly with latitude and temperature, since temperature is the dominant control on forest phenology. In contrast, phenology transition dates for shrubs, savannas, and grasses, especially in Europe and Asia, exhibit

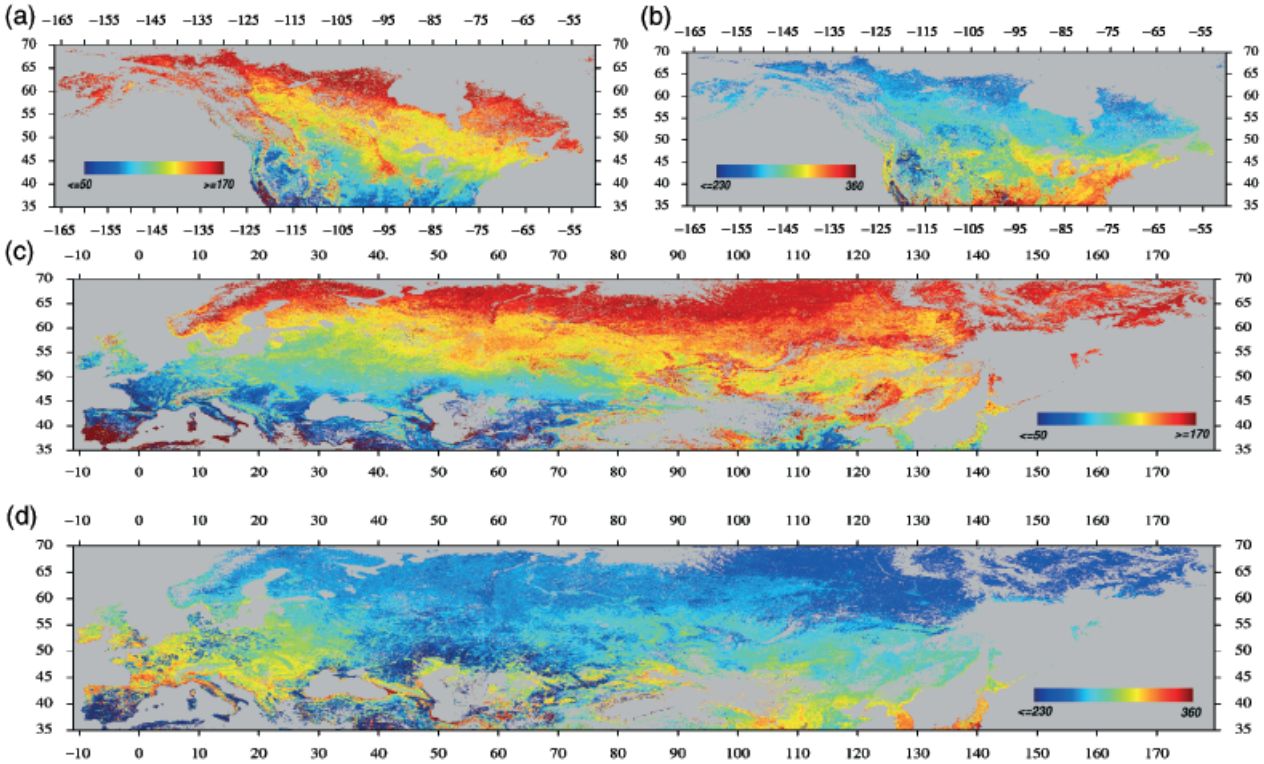

Fig. 2 Spatial patterns of vegetation phenology in 2001. Only the first cycle is displayed for pixels with multiple modes. The color legend indicates the day of year while the gray indicates the areas either without vegetation or without good quality of temporal data. The horizontal axis represents the longitude degree and the vertical axis represents latitude degree. (a) Greenup onset in North America, (b) dormancy onset in North America, (c) greenup onset in Europe and Asia, and (d) dormancy onset in Europe and Asia.

relatively little dependence on latitude and temperature below roughly 45°N because seasonal variation in phenology in these regions is controlled by water availability. In general, the relationship between phenology and latitude is less variable in North America than in Europe and Asia. This difference is likely caused by water limitations, which are more geographically extensive in Europe and Asia than in North America.

Crop greenup exhibits similar patterns to other land-cover types with respect to temperature regimes and latitude, but human activity introduces substantial differences. For example, the onset of greenup for crops in the northern central United States (about 43°N and northward) occurs about 5 days later on average than in adjacent forests. However, crop phenology is quite variable and depends strongly on crop type and human management.

Dependence of phenological transition dates on latitude and surface temperature

Figures 3 and 4 also illustrate the dependence of phenology on temperature and latitude. Table 1 summarizes the corresponding trends in greenup and dormancy as a function of latitude, and demonstrates the sensitivity of vegetation phenology to environmental parameters estimated through linear regression models. The regression models are all strongly significant ($P < 0.0001$) based on sample sizes ranging from 715 to 2073 for each of the various land-cover types. The goodness of fit (R^2) is larger than 0.8, with the exception of urban areas in North America.

The rate of change in greenup and dormancy onsets as a function of latitude indicates that the phenological events vary by about 2 days per degree of latitude in North America, Europe, and Asia. Generally, the rate of change in greenup onset is greater than in dormancy onset for most land-cover types. The rate of northward progression in greenup onset in this study is smaller than that derived by Hopkins (1938; Reader *et al.*, 1974) who proposed that the average value is 4 days per degree of latitude. As noted by Fitzjarrald *et al.* (2001), however, phenological progress with latitude is not uniform because of complexity introduced by climate and land-cover types.

Table 2 shows the mean rate of change in GSL as a function of mean annual LST. These results indicate that forests are again the most sensitive to temperature

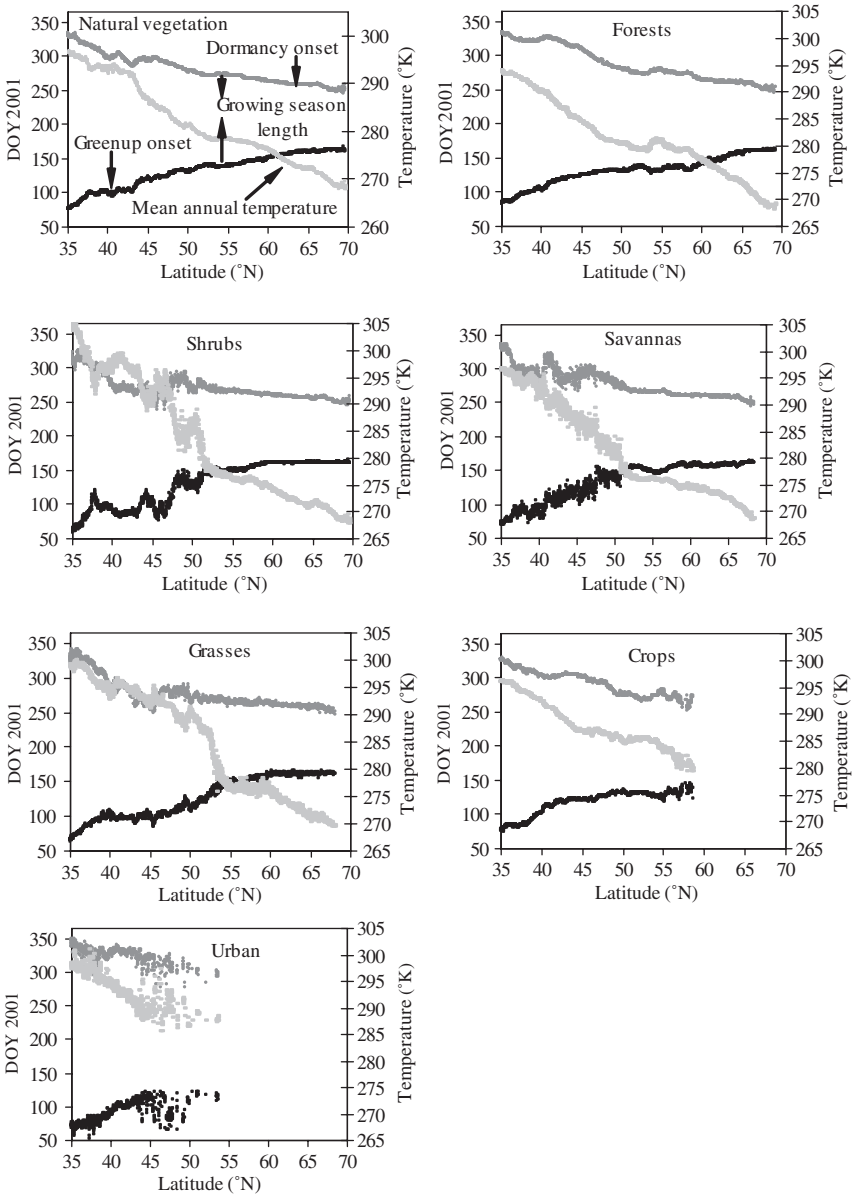

Fig. 3 Vegetation phenology as a function of land-cover type, latitude and land surface temperature (LST) in North America. Black dots are greenup onset, dark gray dots are dormancy onset, and light gray dots are LST.

variations, followed by savannas. The dependence is lower for shrubs and grasses, and urban areas respond in a fashion similar to savannas. The overall rate of change in natural vegetation is about 5 days per °C, although this value is slightly larger in North America than in Europe and Asia. This rate is very similar to the change in GSL inferred for deciduous broadleaf forests associated with the increases in mean annual temperature during the twentieth century (White *et al.*, 1999). However, the change rates in this study are much smaller than the results derived from time series of AVHRR NDVI, where GSL in high-latitude northern hemisphere was inferred to have increased by 12 ± 4 days between 1981 and 1991 (Myneni *et al.*, 1997), by 18 days in Europe and Asia, and by 12 days in northern North America between 1981 and 1999 (Zhou *et al.*, 2001). These results are attributed to global warming, in which the northern high latitudes have warmed by about 0.8 °C since the early 1970s, although the trend is not uniform in all areas (Hansen *et al.*, 1999). The discrepancy between this study and previous findings probably results from several sources. In particular, the dependence on temperature estimated from spatial variation may not be directly comparable with rates inferred from time series data. On the other hand, the estimated changes in GSL from temporal AVHRR

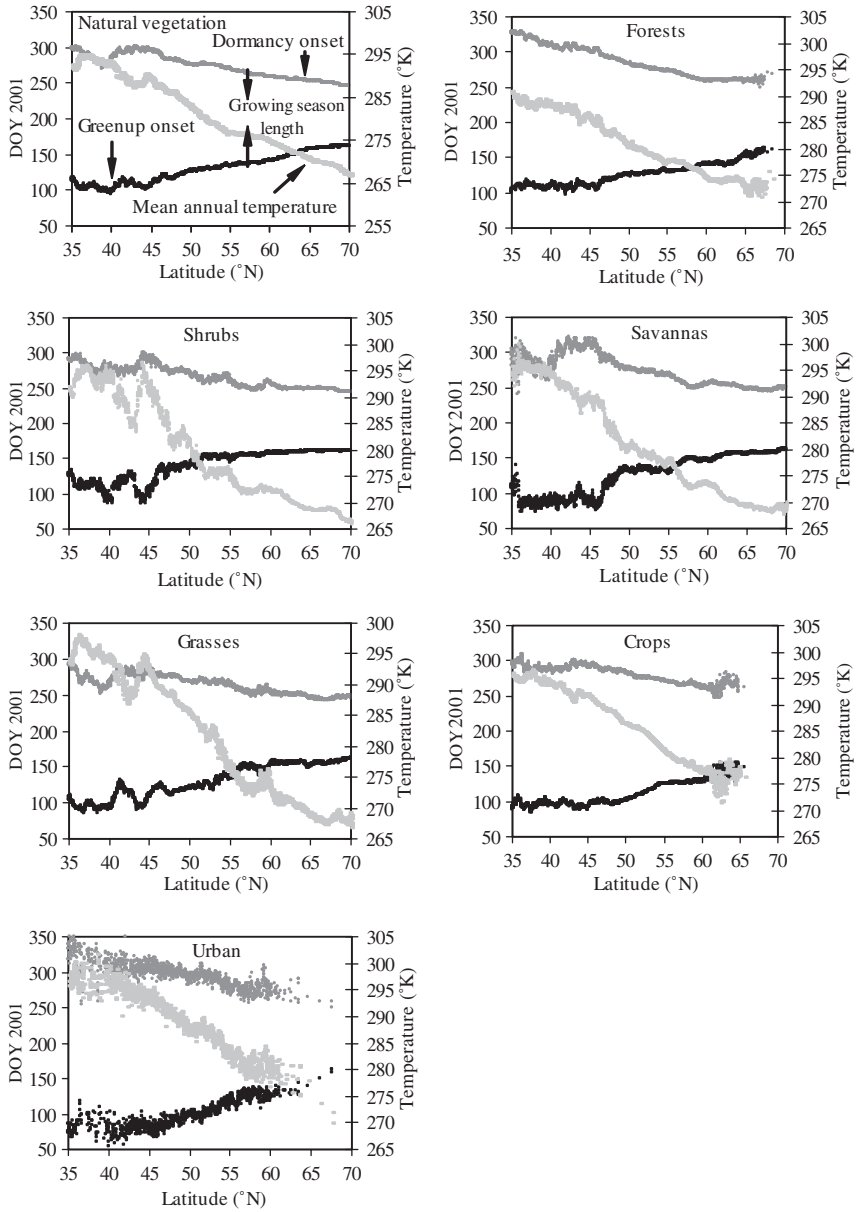

Fig. 4 Vegetation phenology as a function of land-cover type, latitude and land surface temperature (LST) in Europe and Asia. Black dots are greenup onset, dark gray dots are dormancy onset, and light gray dots are LST.

NDVI data were obtained using a fixed threshold to define the growing season, which likely introduces some uncertainty.

Comparison of vegetation phenology between urban and rural areas

Tables 3 and 4 show that greenup onset occurs consistently earlier and dormancy onset occurs later in urban areas relative to other land-cover types in surrounding rural areas for North America, Europe and Asia. Differences in greenup onset (ΔG_d) between urban areas and forests are larger than differences between urban areas and all other land-cover types, whereas the converse is true for the difference in dormancy onset (ΔD_d) for the same classes. In addition, ΔG_d is much larger than ΔD_d for forests, while the converse is true for the other land-cover types. Finally, both ΔG_d and ΔD_d for forests are larger in North America than in Europe and Asia. Conversely, both are smaller for grasses.

Relative to other land-cover types, LST in urban areas was about 1–3 °C higher for both average spring values (January to May) and annual average values (Tables 3

Table 1 Rate of change (days per latitude degree) in phenological events with latitude in North America (35–70°N), and Europe and Asia (40–70°N)

Land-cover type		Natural vegetation	Forests	Shrubs	Savannas	Grasses	Crops	Urban
North America	Greenup	2.31	1.95	2.94	2.67	3.00	2.27	2.39
	Dormancy	−2.07	−2.52	−1.26	−1.84	−1.79	−2.53	−2.08
Europe and Asia	Greenup	2.37	1.80	2.04	2.75	2.13	2.23	3.05
	Dormancy	−2.19	−1.41	−2.22	−1.35	−1.48	−1.97	−2.19

Table 2 Rate of change (day/ °C) in vegetation growing-season length (day) as a function of mean annual land surface temperature (°C) in North America (35–70°N), and Europe and Asia (40–70°N)

Land-cover type	Natural vegetation	Forests	Shrubs	Savannas	Grasses	Crops	Urban
North America	5.303	6.656	3.925	5.151	4.613	7.598	5.152
Europe and Asia	4.662	6.362	3.958	5.786	3.65	4.528	5.792

Table 3 Average differences in both vegetation phenological transition dates and land surface temperature between urban areas and other land-cover types in North America

Difference	Forests	Shrubs	Savannas	Grasses	Crops
Greenup onset (ΔG_d)	−9.1	−7.6	−5.2	−4.1	−7.2
Dormancy onset (ΔD_d)	3.9	14.6	7.2	11.2	12.4
Spring temperature (ΔT_{1-5})	3.0	2.4	2.3	2.1	2.1
Annual temperature (ΔT_a)	3.2	1.8	2.4	1.7	2.1

Table 4 Average differences in both vegetation phenological transition dates and temperature between urban areas and other land-cover types in Europe and Asia

Difference	Forests	Shrubs	Savannas	Grasses	Crops
Greenup onset (ΔG_d)	−7.4	−5.1	−5.7	−6.0	−4.3
Dormancy onset (ΔD_d)	2.5	14.7	5.8	16.5	10.5
Spring temperature (ΔT_{1-5})	2.2	2.0	2.0	1.7	1.1
Annual temperature (ΔT_a)	2.6	1.6	2.3	1.1	1.1

and 4). LST differences between urban and natural vegetation both in spring (ΔLST_{1-5}) and annually (ΔLST_a) are larger in North America than in Europe and Asia, where the maximum differences are 0.8 °C. This result shows that urbanization exerts considerable control on temperature regimes, which in turn drives

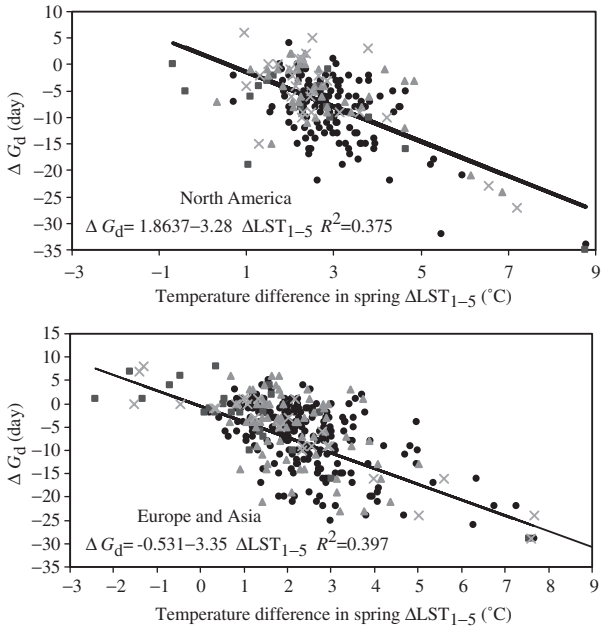

Fig. 5 Land-cover-specific differences in greenup onset (ΔGd) as a function of differences in spring land surface temperatures in North America (upper panel), and Europe and Asia (lower panel). (●) Urban vs. forests, (■) urban vs. shrubs, (▲) urban vs. savannas, (×) urban vs. grasses.

early greenup onset and late dormancy onset. It also indicates that the effect of urbanization is stronger in North America than in Europe and Asia. This difference might be attributed to the denser and taller configuration of cities in the United States relative to European cities (Bonnan, 2002).

Figure 5 reveals that ΔG_d between urban and naturally vegetated areas is a function of temperature

differences in the spring (ΔLST_{1-5}). Linear regression indicates that the relationship is highly significant ($R^2 = 0.38$ and t-test = 15.30 in North America, and $R^2 = 0.40$ and t-test = 14.6 in Europe and Asia) although there is ample scatter present in this relationship, which may be caused by complicating effects such as water availability, especially in grasslands and shrublands. In general, the linear relationship between ΔG_d and ΔLST_{1-5} indicates that a 1 °C increase in ΔLST_{1-5} results in greenup onset occurring about 3 days earlier in North America, Europe and Asia. This rate of change in greenup onset is closely comparable with values (3–4 days per °C) measured from field observations (Fitter *et al*., 1995; Kramer, 1996; Rötzer & Chmielewski, 2000).

Differences in vegetation growing-season length (ΔGSL) between urban and other land-cover types exhibit land-cover dependent relationships with mean annual temperature (ΔLST_a) (Fig. 6). Similar results were obtained when ΔLST_a was replaced with the difference in mean temperature during growing season. Specifically, a weak linear trend is detectable for ΔGSL between urban vegetation and natural forests in North America, Europe, and Asia. However, this effect is not significant for shrubs, savannas, and grasses. It is likely that shrubs and grasses are affected more strongly by water availability than forests during the growing season. In addition, this result may reflect the fact that the end of the growing season is controlled by both photoperiod and temperature (Hänninen *et al*., 1990; Schwartz, 1990).

Thermal time-chilling model of forest greenup onset

To investigate the dependence of vegetation phenology on changes in LST, we tested the ability of Eqn (4) to predict the timing of forest greenup onset. We chose this variable because forests are more strongly driven by temperature than other land-cover types in the mid- to high latitudes. To do this, both DDs and the number of chilling days from dormancy onset to greenup onset were calculated for all forested land areas in the northern hemisphere. Because the thermal time-chilling model is only relevant for regions with sufficient seasonality in temperature, this model was estimated for mid-latitude areas of North America (37–67°N) and for Europe and Asia (40–67°N). The results show that more than 83% of the variation in thermal time (T_{DD}) required for greenup onset can be explained using the thermal time-chilling model when a LST threshold of 5 °C is used. When a LST threshold of 0 °C was used, the model was able to explain 96% and 94% of the variation in thermal time in North America and Europe and Asia, respectively (Fig. 7).

According to established thermal time-chilling models, the duration of chilling should decrease as a result of climate warming, and in turn, the thermal time required for greenup onset should increase. Thus, global warming may act to delay or advance forest greenup onset, depending on the extent to which the chilling and thermal time requirements are currently met. The established models show that the minimum

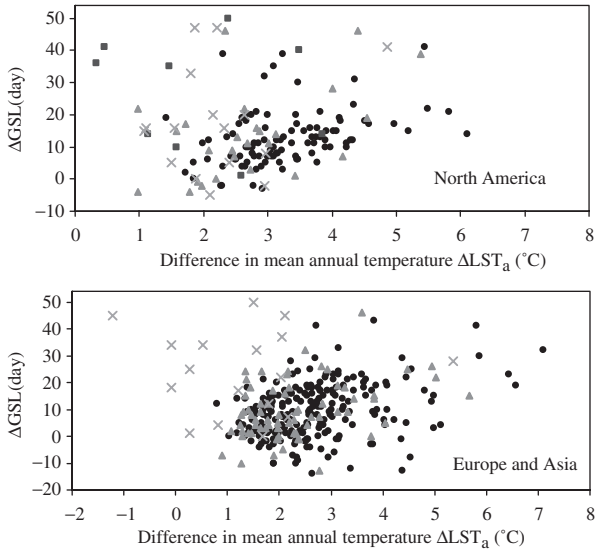

Fig. 6 Differences between urban and other land-cover types in vegetation growing-season length (DGSL) as a function of mean annual land surface temperature (ΔLSTa) for North America, and Europe and Asia. (•) Urban vs. forests, (■) urban vs. shrubs, (▲) urban vs. savannas, (×) urban vs. grasses.

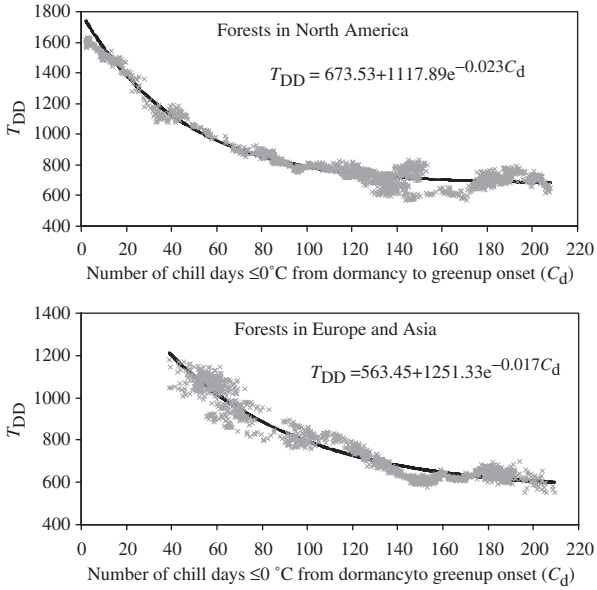

Fig. 7 Relationship between the thermal time to greenup onset and the accumulated number of chill days for forests in the mid- to high latitudes of North America, Europe and Asia. TDD is degree days (>0 °C) from dormancy onset to greenup onset.

requirement for T_{DD} is 563°C in Europe and Asia and 673°C in North America. When C_d is larger than about 120 days (48°N and northward) in North America and 140 days (52°N and northward) in Europe and Asia, T_{DD} mainly fluctuates within $563 \pm 100^{\circ}$ and $673 \pm 100^{\circ}$. In these regions, chilling requirements are far exceeded. Therefore, any decrease in chilling days caused by global warming will have little or no effect on T_{DD}, and greenup onset should advance with climate warming. In contrast, in the regions where T_{DD} decreases rapidly with increasing C_d (e.g. in the mid-latitudes with low C_d), the chilling requirements are nearly exactly sufficient at present and slight reductions in C_d may result in a large increase in thermal time requirements. Climate warming should therefore cause an increase in T_{DD} requirements, so that advances in greenup onset will be limited or even inverted. This type of pattern is similar to the species-level results described by Cannell & Smith (1986) in the Scottish uplands. Moreover, this finding is also supported by observed trends in the onset of spring in recent decades inferred from Bowen ratio data in the Eastern United States (Fitzjarrald *et al*., 2001). Specifically, the results described by Fitzjarrald *et al*. (2001) show that spring dates advanced by 6–8 days in northeastern areas, and that the amount of change decreased towards the south where spring actually occurred later in southern areas of Virginia and the Carolinas.

Discussion and conclusions

This paper has explored spatial and temporal patterns of vegetation phenology and their relationships with both LST and land-cover type in the mid- to high latitudes of the northern hemisphere in 2001 using MODIS data. In this context, it is important to note that the analysis in this paper used only 1 year's worth of data. Therefore, phenological trends might vary slightly with data for different years. The results show that phenological variations correlate strongly with both LST and latitude for all land-cover types. On average, greenup onset moves northward and dormancy onset spreads southward at a rate of about 2 days per degree of latitude, although the rates are slightly higher for greenup onset than for dormancy onset. Because forests dominate humid ecosystems, while shrubs and grasses are associated with relatively dry ecosystems, phenological transition dates in forests show the strongest dependence on latitude and temperature. The rate of change in GSL as a function of mean annual LST is highest in forests (6.4 days per °C in Europe and Asia, and 6.7 days per °C in North America), followed by savannas, shrubs, and grasses.

The effect of urban climates on phenology is also shown to be significant in the northern hemisphere. Average LSTs in urban areas are about 1–3 °C higher than surrounding rural areas, with larger differences observed in North America than in Europe and Asia. On average, the result of urban climates leads to an advance in greenup onset (about 3 days per °C) and a delay in dormancy onset, although the magnitude of this effect is quite variable. Note that the differences observed in this study were obtained from cells that are $0.5 \times 0.5^{\circ}$ with a conservative threshold used to define urban areas. To pursue this question more fully, it might be more appropriate to investigate the effects of urban climate using individual urban areas.

This research also estimated empirical models to explain the behavior of greenup onset in forests of North America, Europe, and Asia. The model results suggest that greenup onset is sensitive to global warming from about 48°N northward in North America and from about 52°N northward in Europe and Asia, with diminished sensitivity in lower latitudes. However, to extrapolate these results to global scales and accurately predict the effect of global warming on vegetation phenology, the model needs to be evaluated using independent data from different years. Moreover, to fully evaluate the sensitivity of global ecosystems to climate change, models of greenup onset applicable to other land-cover types need to be investigated.

Finally, it should be noted that the results presented in this paper are somewhat dependent on the temporal and spatial resolution of the MODIS NBAR data. Specifically, because the NBAR EVI data are representative of 16-day periods, the estimated phenological transition dates can possess substantial uncertainty. At the same time, the method used is unbiased, and the zonal averages considered in this paper should therefore be robust. In the near future, the temporal resolution of NBAR data will increase to 1 day, which should increase the accuracy of phenological retrievals accordingly.

Within this framework, the quality of EVI data, especially as it relates to the frequency of missing data during the periods when vegetation growth transitions from one stage to another, can strongly influence estimates of phenological events and further analysis is needed to assess how EVI quality and missing data affect retrievals. Further, since each 1 km pixel generally consists of several cover types or species, it is important to acknowledge that the phenological events identified in this research are representative of vegetation communities, rather than individual species.

In the context of global change processes, quantification of this type of ecosystem-level response should provide a useful and important complement to

species-level studies. Indeed, a key challenge confronting the global change community is better understanding regarding how species-level responses to climate forcing aggregate to larger scales. The type of remote sensing-based analysis presented in this paper, when linked to carefully designed field-based studies, provides a promising approach for tackling this issue.

Acknowledgements

This work was funded under NASA contract, NAS5-31369.

References

Beaubien EG, Freeland HJ (2000) Spring phenology trends in Alberta, Canada: links to ocean temperature. *Internal Journal of Biometeorol*, **44**, 53–59.

Bonnan G (2002) *Ecological Climatology – Concepts and Applications*. Cambridge University Press, Cambridge.

Botta A, Viovy N, Ciais P *et al*. (2000) A global prognostic scheme of leaf onset using satellite data. *Global Change Biology*, **6**, 709–725.

Cannell MGR, Murray MB, Sheppard LJ (1985) Forest avoidance by selection for late budburst in *Picea Sitchensis*. *Journal of Applied Ecology*, **22**, 931–941.

Cannell MGR, Smith RI (1983) Thermal time, chill days and prediction of budburst in *Picea sitchensis*. *Journal of Applied Ecology*, **20**, 951–963.

Cannell MGR, Smith RI (1986) Climatic warming, spring budbursts, and forest damage on trees. *Journal of Applied Ecology*, **23**, 177–191.

Chmielewski F-M, Rötzer T (2001) Response of tree phenology to climate change across Europe. *Agricultural and Forest Meteorology*, **180**, 101–112.

Duchemin B, Goubier J, Courrier G (1999) Monitoring phenological key stages and cycle duration of temperate deciduous forest ecosystems with NOAA/AVHRR data. *Remote Sensing of Environment*, **67**, 68–82.

Emberlin J, Detandt M, Gehrig R *et al*. (2002) Responses in the start of Betula (birch) pollen seasons to recent changes in spring temperatures across Europe. *International Journal of Biometeorology*, **46**, 159–170.

Fisher A (1994) A model for the seasonal variations of vegetation indices in coarse resolution data and its inversion to extract crop parameters. *Remote Sensing of Environment*, **48**, 220–230.

Fitter AH, Filtter RSR, Harris ITB *et al*. (1995) Relationship between first flowering date and temperature in the flora of a locality in central England. *Functional Ecology*, **9**, 55–60.

Fitzjarrald DR, Acevedo OC, Moore KE (2001) Climatic consequences of leaf presence in the eastern United States. *Journal of Climate*, **14**, 598–614.

Franken E (1955) Der Beginn der Forsythienbluete in Hamberg 1955. *Meteorologische Rundschau*, **8**, 113–115.

Friedl MA, McIver DK, Hodges JCF *et al*. (2002) Global land cover mapping from MODIS: algorithms and early results. *Remote Sensing of Environment*, **83**, 287–302.

Goward SN, Markham B, Dye DG *et al*. (1991) Normalized difference vegetation index measurements from the advanced very high resolution radiometer. *Remote Sensing of Environment*, **35**, 257–277.

Gutzler DS, Rosen RD (1992) Internal variability of wintertime snow cover across the northern-hemisphere. *Journal of Climate*, **5**, 1441–1447.

Hänninen H, Hkkinen R, Hari P *et al*. (1990) Timing of growth cessation in relation to climatic adaptation of northern woody plants. *Tree Physiology*, **6**, 29–39.

Hansen J, Ruedy R, Glascoe J (1999) GISS analysis of surface temperature change. *Journal of Geophysical Research – Atmospheres*, **104**, 30997–31022.

Hopkins AD (1938) Bioclimatics – A science of life and climate relations. *US Department of Agriculture Misc. Publication No. 280*. US Government Printing Office, Washington, DC.

Huband NDS, Monteith JL (1986) Radiative surface temperature and energy balance of a wheat canopy. *Boundary-Layer Meteorology*, **36**, 1–17.

Huete A, Didan K, Miura T *et al*. (2002) Overview of the radiometric and biophysical performance of the MODIS vegetation indices. *Remote Sensing of Environment*, **83**, 195–213.

Hunter AF, Lechowicz MJ (1992) Predicting the timing of budburst in temperate trees. *Journal of Applied Ecology*, **29**, 597–604.

Justice CO, Vermote E, Townshend JRG *et al*. (1997) The moderate resolution imaging spectroradiometer (MODIS): land remote sensing for global change research. *IEEE Transactions on Geoscience and Remote Sensing*, **36**, 1228–1249.

Kramer K (1994) Selecting a model to predict the onset of growth of *Fagus sylvatica*. *Journal of Applied Ecology*, **31**, 172–181.

Kramer K (1996) *Phenology and growth of European trees in relation to climate change*. Thesis, Landbouw Universiteit Wageningen.

Lauscher F (1978) Neue Analysen ältester und neuerer phänologischer Reihen. *Arch. für Meteorologie, Geophysik und Klimatologie (Ser. B)*, **26**, 373–385.

Lechowicz MJ, Koike T (1995) Phenology and seasonality of woody plants: an unappreciated element in global change research? *Canadian Journal of Botany*, **73**, 175–182.

Lieth H (1975) Modeling the primary productivity of the World. In: *Primary Productivity of the Biosphere. Ecology Studies 14* (eds Lieth H, Whitttaker RH), Springer, Berlin pp. 237–264.

Linkosalo T (2000) Mutual regularity of spring phenology of some boreal tree species: predicting with other species and phenological models. *Canadian Journal of Forest Research*, **30**, 667–673.

Lloyd D (1990) A phenological classification of terrestrial vegetation cover using shortwave vegetation index imagery. *International Journal of Remote Sensing*, **11**, 2269–2279.

Lucht W, Prentice IC, Myneni RB *et al*. (2002) Climatic control of the high-latitude vegetation greening trend and Pinatubo effect. *Science*, **296**, 1687–1689.

Markon CJ, Fleming MD, Binnian EF (1995) Characteristic of vegetation phenology over the Alaskan landscape using AVHRR time-series data. *Polar Record*, **31**, 179–190.

Moulin S, Kergoat L, Viovy N *et al*. (1997) Global-scale assessment of vegetation phenology using NOAA/AVHRR satellite measurements. *Journal of Climate*, **10**, 1154–1170.

Myneni RB, Keeling CD, Tucker CJ *et al*. (1997) Increased plant growth in the northern high latitudes from 1981–1991. *Nature*, **386**, 698–702.

Parmesan C, Yohe G (2003) A globally coherent fingerprint of climate change impacts across natural systems. *Nature*, **421**, 37–42.

Press WH, Teukolsky SA, Vetterling WT (1997) *Numerical Recipes in C – The Art of Scientific Computing*, 2nd edn. Cambridge University Press, Cambridge pp. 656–688.

Ratkowsky DA (1983) *Nonlinear Regression Modeling – A Unified Practical Approach*. Marcel Dekker, New York and Basel pp. 61–91.

Reader R, Radford JS, Lieth H (1974) Modeling important phytophenological events in eastern North America. In: *Phenology and Seasonality Modeling* (ed. Lieth H), Springer, New York pp. 329–342.

Reed BC, Brown JF, VanderZee D *et al*. (1994) Measuring phenological variablity from satellite imagery. *Journal of Vegetation Science*, **5**, 703–714.

Roetzer T, Wittenzeller M, Haechel H *et al*. (2000) Phenology in central Europe-differences and trends of spring phenophases in urban and rural areas. *International Journal of Biometeorology*, **44**, 60–66.

Rötzer T, Chmielewski FM (2000) Phenological maps of Europe. *Agrarmeteorologische Schriften*, **H6**, 1–12.

Sarvas R (1974) Investigations on the annual cycle of development of forest tree autumn dormancy and winter dormancy. *Communicationes Instituti Forestalis Fenniae*, **84**, 1–101.

Schaaf CB, Gao F, Strahler AH *et al*. (2002) First operational BRDF, Albedo and Nadir reflectance products from MODIS. *Remote Sensing of Environment*, **83**, 135–148.

Schwartz MD (1990) Detecting the onset of spring: a possible application of phenological models. *Climate Research*, **1**, 23–29.

Schwartz MD (1999) Advancing to full bloom: planning phenological research for the 21st century. *International Journal of Biometeorology*, **42**, 113–118.

Spano D, Cesaraccio C, Duce P *et al*. (1999) Phenological stage of natural species and their use as climate indicators. *International Journal of Biometeorology*, **42**, 124–133.

Sparks TH, Carey PD (1995) The responses of species to climate over 2 centuries – an analysis of the Marsham phonological record, 1736–1947. *Journal of Ecology*, **83**, 321–329.

Wan ZM, Zhang YL, Zhang QC *et al*. (2002) Validation of the land-surface temperature products retrieved from terra moderate resolution imaging spectroradiometer data. *Remote Sensing of Environment*, **83**, 163–180.

White MA, Nemani RN, Thornton PE *et al*. (2002) Satellite evidence of phenological difference between urbanized and rural areas of the eastern United States deciduous broadleaf forest. *Ecosystems*, **5**, 260–277.

White MA, Running SW, Thornton PE (1999) The impact of growing-season length variability on carbon assimilation and evapotranspiration over 88 years in the eastern US deciduous forest. *International Journal of Biometeorology*, **42**, 139–145.

White MA, Thornton PE, Running SW (1997) A continental phenology model for monitoring vegetation responses to interannual climatic variability. *Global Biogeochemical Cycles*, **11**, 217–234.

Zhang X, Friedl MA, Schaaf CB *et al*. (2003) Monitoring vegetation phenology using MODIS. *Remote Sensing of Environment*, **84**, 471–475.

Zhou L, Tucker CJ, Kaufmann RK *et al*. (2001) Variation in northern vegetation activity inferred from satellite data of vegetation index during 1981 to 1999. *Journal of Geophysical Research*, **106**, 20069–20083.